รายการอ้างอิง

1. A. F. Frangi, W. J. Niessen and M. A. Viergever. Three-dimensional modeling for functional analysis of cardiac images: A review. IEEE Transactions on Medical Imaging 20 (January 2001): 2-25.
2. G. Stalidis, N. Maglaveras, S. N. Efstratiadis, A. S. Dimitriadis and C. Pappas. Model-based processing scheme for quantitative 4-D cardiac MRI analysis. IEEE Transactions on Information Technology in Biomedicine 6 (March 2002): 59-72.
3. M. Kass, A. Witkin and D. Terzopoulos. Snakes: Active contour models. International Journal of Computer Vision 1 (1988): 321–331.
4. C. Xu and J. L. Prince. Snakes, shapes, and gradient vector flow. IEEE Transactions on Image Processing 7 (March 1998): 359–369.
5. J. Cheng and S. W. Foo. Dynamic directional gradient vector flow for snakes. IEEE Transactions on Image Processing 15 (June 2006): 1563–1571.
6. II.-H. Shin, M.-J. Kwon, S.-T Chung and H. W. Park. Segmentation and visualization of left ventricle in MR cardiac images. IEEE International Conference on Image Processing 2 (September 2002): 89-92.
7. C. Zimmer and J.-C. Olivo-Marin. Coupled parametric active contours. IEEE Transactions on Pattern Analysis and Machine Intelligence 27 (November 2005): 1838-1842.
8. T. F. Chan and L. A. Vese. Active contours without edges. IEEE Transactions on Image Processing 10 (Febuary 2001): 266–277.
9. C. Pluempitiwiriyawej, J. M. F. Moura, Y.-J. L. Wu and C. Ho. STACS: New active contour scheme for cardiac MR image segmentation. IEEE Transactions on Medical Imaging 24 (May 2005): 593-603.
10. C. Pluempitiwiriyawej, J. M. F. Moura, Y.-J. L. Wu and C. Ho. Cardiac MR image segmentation: Quality assessment of STACS. IEEE International Symposium on Biomedical Imaging 1 (April 2004): 828-831.
11. C. Pluempitiwiriyawej, J. M. F. Moura, Y.-J. L. Wu, S. Kanno and C. Ho. Stochastic active contour for cardiac MR image segmentation. IEEE International Conference on Image Processing 1 (September 2003): 1097-1100.

12. C. Pluempitiwiriyawej and S. Sotthivirat. Active contours with automatic initialization for myocardial perfusion analysis. IEEE Proceedings Conference of the Engineering in Medicine and Biology Society (September 2005): 3332-3335.

13. A. Tsai, A. Yezzi, W. Wells, C. Tempany, D. Tucker, A. Fan, W. E. Grimson and A. Willsky. A shape-based approach to the segmentation of medical imagery using level sets. IEEE Transactions on Medical Imaging 22 (February 2003): 137-154.

14. Q. Chen, Z. M. Zhou, M. Tang, P. A. Heng and D.-S. Xia. Shape statistics variational approach for the outer contour segmentation of left ventricle MR images. IEEE Transactions on Information Technology in Biomedicine 10 (July 2006): 588-597.

15. R. Malladi, J. Sethian and B. C. Vemuri. Shape modeling with front propagation: a level set approach. IEEE Transactions on Pattern Analysis and Machine Intelligence 17 (February 1995): 158-175.

16. สุทธิศักดิ์ สุทธิพงษ์ชัย. เตรียมพร้อมก่อนตรวจ MRI[online]. แหล่งที่มา : http://www.si.mahidol.ac.th/sidoctor/month/sidoctor2004/mar04_MRI.htm [1 พฤศจิกายน 2549]

17. Heart Anatomy[online]. Available form : http://texasheart.org/HIC/Anatomy/anatomy2.cfm [2006, November 1]

18. A. P. Zijdenbos, B. M. Dawant, R. A. Margolin and C. Palmer. Morphometric anaysis of white matter lesions in MR images: Method and validation. IEEE Transactions on Medical Imaging 3 (December 1994): 716–724.

19. M. Stella Atkins and B. T. Mackiewich. Fully automatic segmentation of the brain in MRI. IEEE Transactions on Medical Imaging 17 (February 1998): 98–107.

ภาคผนวก

ภาคผนวก ก
ที่มาของสมการแรงระหว่างคอนทัวร์

ในบทที่ 3 หัวข้อที่ 3.2.2 ได้มีการออกแบบและทดสอบความสามารถของแรงระหว่างคอนทัวร์ โดยใช้สมการที่ (3.4) และ (3.5) ซึ่งพจน์ที่สามของสมการทั้งสองนี้ คือ แรงระหว่างคอนทัวร์ โดยมีที่มาจากการทำให้ฟังก์ชันพลังงานระหว่างคอนทัวร์ในสมการที่ (ก.1) มีค่าน้อยที่สุด ด้วยการหาอนุพันธ์ของสมการที่ (ก.1) เทียบกับฟังก์ชัน C_A และ C_B ตามลำดับ

$$E_{\text{inter}}(C_A, C_B) = \nu\left(\|C_A - C_B\| - r\right)^2 \qquad \text{(ก.1)}$$

โดยที่ C_A และ C_B คือ คอนทัวร์ A และ คอนทัวร์ B ตามลำดับ, ν คือ ค่าคงที่บวก ทำหน้าที่เป็นตัวถ่วงน้ำหนัก และ r คือ ระยะห่างระหว่างคอนทัวร์ทั้งสองที่เราต้องการ ผลของการหาอนุพันธ์ของสมการที่ (ก.1) เทียบกับฟังก์ชัน C_A และ C_B ได้ดังสมการที่ (ก.2) และ (ก.3) ตามลำดับ

$$\frac{\partial E_{\text{inter}}}{\partial C_A} = 2\nu\left(\|C_A - C_B\| - r\right)\frac{\partial}{\partial C_A}\|C_A - C_B\| \qquad \text{(ก.2)}$$

$$\frac{\partial E_{\text{inter}}}{\partial C_B} = 2\nu\left(\|C_A - C_B\| - r\right)\frac{\partial}{\partial C_B}\|C_A - C_B\| \qquad \text{(ก.3)}$$

โดยที่ $\|C_A - C_B\|$ คือ ระยะห่างระหว่างคอนทัวร์ A และ คอนทัวร์ B ซึ่งสามารถคำนวณได้จากสมการที่ (ก.4)

$$\|C_A - C_B\| = \sqrt{(x_A - x_B)^2 + (y_A - y_B)^2} \qquad \text{(ก.4)}$$

โดยที่ (x_A, y_A) และ (x_B, y_B) คือ คู่อันดับของจุดบนคอนทัวร์ A และ คอนทัวร์ B ตามลำดับ ดังนั้นเราสามารถคำนวณค่า $\frac{\partial}{\partial C_A}\|C_A - C_B\|$ ในสมการที่ (ก.2) ได้โดยแยกการคำนวณออกเป็นสองสมการ คือ การหาอนุพันธ์เทียบกับ x_A และ y_A ดังสมการที่ (ก.5) และ (ก.6)

$$\frac{\partial\|C_A - C_B\|}{\partial x_A} = \frac{(x_A - x_B)}{\sqrt{(x_A - x_B)^2 + (y_A - y_B)^2}} = \frac{(x_A - x_B)}{\|C_A - C_B\|} \quad (ก.5)$$

$$\frac{\partial\|C_A - C_B\|}{\partial y_A} = \frac{(y_A - y_B)}{\sqrt{(x_A - x_B)^2 + (y_A - y_B)^2}} = \frac{(y_A - y_B)}{\|C_A - C_B\|} \quad (ก.6)$$

จากสมการที่ (ก.5) และ (ก.6) ทำให้ได้ค่า $\frac{\partial}{\partial C_A}\|C_A - C_B\|$ ดังสมการที่ (ก.7)

$$\frac{\partial\|C_A - C_B\|}{\partial C_A} = \frac{(C_A - C_B)}{\|C_A - C_B\|} \quad (ก.7)$$

และสามารถคำนวณค่า $\frac{\partial}{\partial C_B}\|C_A - C_B\|$ ในสมการที่ (ก.3) ได้โดยแยกการคำนวณออกเป็นสองสมการ คือ การหาอนุพันธ์เทียบกับ x_B และ y_B ดังสมการที่ (ก.8) และ (ก.9)

$$\frac{\partial\|C_A - C_B\|}{\partial x_B} = \frac{(x_B - x_A)}{\sqrt{(x_A - x_B)^2 + (y_A - y_B)^2}} = \frac{(x_B - x_A)}{\|C_A - C_B\|} \quad (ก.8)$$

$$\frac{\partial\|C_A - C_B\|}{\partial y_B} = \frac{(y_B - y_A)}{\sqrt{(x_A - x_B)^2 + (y_A - y_B)^2}} = \frac{(y_B - y_A)}{\|C_A - C_B\|} \quad (ก.9)$$

จากสมการที่ (ก.8) และ (ก.9) ทำให้ได้ค่า $\frac{\partial}{\partial C_B}\|C_A - C_B\|$ ดังสมการที่ (ก.10)

$$\frac{\partial\|C_A - C_B\|}{\partial C_B} = \frac{(C_B - C_A)}{\|C_A - C_B\|} \quad (ก.10)$$

แทนสมการที่ (ก.7) เข้าไปในสมการที่ (ก.2) จะได้ $\frac{\partial E_{inter}}{\partial C_A}$ ดังสมการที่ (ก.11)

$$\begin{aligned}\frac{\partial E_{inter}}{\partial C_A} &= 2\nu\left(\|C_A - C_B\| - r\right)\frac{(C_A - C_B)}{\|C_A - C_B\|} \\ &= 2\nu(C_A - C_B)\left[1 - \frac{r}{\|C_A - C_B\|}\right]\end{aligned} \quad (ก.11)$$

แทนสมการที่ (ก.10) เข้าไปในสมการที่ (ก.3) จะได้ $\frac{\partial E_{\text{inter}}}{\partial C_{\text{B}}}$ ดังสมการที่ (ก.12)

$$\begin{aligned}\frac{\partial E_{\text{inter}}}{\partial C_{\text{B}}} &= 2\nu\left(\left\|C_{\text{A}}-C_{\text{B}}\right\|-r\right)\frac{\left(C_{\text{B}}-C_{\text{A}}\right)}{\left\|C_{\text{A}}-C_{\text{B}}\right\|} \\ &= 2\nu\left(C_{\text{B}}-C_{\text{A}}\right)\left[1-\frac{r}{\left\|C_{\text{A}}-C_{\text{B}}\right\|}\right]\end{aligned} \qquad \text{(ก.12)}$$

ค่าที่ได้ในสมการที่ (ก.11) และ (ก.12) คือ สมการแรงระหว่างคอนทัวร์ ของคอนทัวร์ A และ คอนทัวร์ B ตามลำดับ ซึ่งถูกนำไปใช้ในพจน์ที่สามด้านขาวมือของสมการที่ (3.4) และ (3.5)

ภาคผนวก ข
บทความที่ได้รับการตีพิมพ์

Sopon Phumeechanya and Charnchai Pluempitiwiriyawej, "Left ventricular segmentation using double region-based snakes," The Fourth IEEE International Symposium on Biomedical Imaging (ISBI '07): From Nano to Macro, Washington D.C., USA, 12-15 April 2007.

LEFT VENTRICULAR SEGMENTATION USING DOUBLE REGION-BASED SNAKES

Sopon Phumeechanya and Charnchai Pluempitiwiriyawej

Department of Electrical Engineering, Chulalongkorn University, Bangkok, 10330, Thailand
E-mail: soponpu@yahoo.com and charnchai.P@eng.chula.ac.th

ABSTRACT

We present a double region-based snake method to segment endocardial and epicardial boundaries of the left ventricle in cardiac MR images. The method is based on a region-based parametric active contour. The first active contour is designed to segment the endocardial boundary while the second active contour is to segment the epicardial boundary. We insert the inter-contour forces between the two convolving contours in order to control the distance between them. Our proposed method not only has an ability to segment the endocardial and the epicardial boundaries of the left ventricle simultaneously without requiring any training sets, it is also able to segment cardiac MR images with low contrast between the myocardium and other organs. We initially place both contours within the epicardial boundary of the left ventricle. Furthermore, the problem that one of the contours may, on occasions, be attracted to the boundary of the papillary muscles is solved by checking for the convex hull condition. Our results show successful simultaneous segmentations of the endocardial and the epicardial boundaries, thus the left ventricle of the heart in each MR image.

Index Terms— Active contours, cardiac magnetic resonance imaging, image segmentation, left ventricle, snakes.

1. INTRODUCTION

Left ventricular segmentation in cardiac MR images is a very important process for 3-D or 4-D heart modeling reconstruction [1], which is an essential tool for cardiac diagnosis. The heart models have been used for visualization and deriving functional information, such as the left ventricular mass and the ejection fraction. The left ventricular mass is a predictor of cardiovascular risk and higher mortality [2] while the ejection fraction is a standard medical indicator of a heart's state of health [3]. These reasons justify the necessity to segment the endocardial and the epicardial boundaries (thus the myocardial boundary) of the left ventricle.

One of the widely used segmentation methods, particularly in medical image processing, is active contour or so called "snake" [4]. The contour is defined within the image domain and moves under the influence of internal forces and external forces. The internal forces are imposed on the contour itself in order to control its smoothness while the external forces are usually derived from the image. The curve representation schemes in the active contour literature are broadly classified into parametric active contours [4-7] and geometric active contours [8-11]. Parametric active contours represent curves explicitly in their parametric form while geometric active contours represent curves implicitly as the zero level set of a scalar function [11] over a fixed grid in the image plane.

The external force of an active contour is very essential because it acts as an attractor for the contour to move toward interesting features of the object in the image. There are many types of external force, pure edge-based [4-6], pure region-based [7-8], both edge and region-based [9], and shape-based [10-11]. The drawbacks of pure edge-based external force are that they are very sensitive to noise and the initial contours must start close enough to the actual boundary of the object. On the other hand, the region-based methods perform better than pure edge-based methods when the contrast between the object and the background is low, with an expense of higher computational complexity. Therefore, the hybrid methods that combine both edge and region based information have been proposed [9]. Moreover, to improve the segmentation accuracy, the prior-shape information is often included. Although the shape-based methods have shown many successful segmentation results in various medical images, they need a good training set which must be done manually a priori.

In many segmentation methods for the left ventricle of the heart using active contours, the endocardial and epicardial boundaries are usually treated independently and both active contours perform the segmentation separately [12]. In this paper, however, we design double region-based snakes to track both myocardial boundaries of the left ventricle in a series of cardiac MR images simultaneously. Our method uses region-based parametric active contours [7] because the region-based approach is robustness to noise and the parametric representation is simple to calculate. We also design an inter-contour force to control the distance between both contours so that they do not collapse and become one contour. The first snake is designed to segment endocardial boundary and restricted to be inside the second snake which is aimed to segment epicardial boundary. The initial position of both active contours are placed within the epicardial boundary of left ventricle. The problem of papillary muscles is solved by checking for the

convex hull condition at each iteration while the contours are evolving.

2. SINGLE REGION-BASED SNAKES

We choose the region-based snake for our work. The energy functional of a single region-based snake [7] comprises the internal energy E_{int} and the external energy E_{ext} as in equation (1)

$$\begin{aligned} E(C, R_{\text{in}}, R_{\text{out}}) &= E_{\text{int}} + E_{\text{ext}} \\ &= \tfrac{1}{2}\int_0^1 \left[\alpha\left(\frac{\partial C}{\partial s}\right)^2 + \beta\left(\frac{\partial^2 C}{\partial s^2}\right)^2\right] ds \\ &+ \left[\lambda_{\text{in}}\int_{\overset{\cap}{C}} (I - R_{\text{in}})^2 d\sigma + \lambda_{\text{out}}\int_{\overset{\cup}{C}} (I - R_{\text{out}})^2 d\sigma\right], \quad (1) \end{aligned}$$

where $C(s) = [x(s), y(s)]$, $s \in [0, 1]$, is the contour, $\overset{\cap}{C}$ denotes the region inside C, $\overset{\cup}{C}$ denotes the region outside C, I is the local image intensity, $d\sigma$ is the elementary surface, R_{in} and R_{out} are unknown scalars representing the eventual average intensities inside and outside the contour C, respectively, and α, β, λ_{in}, and λ_{out} are positive constants acting as weighting parameters. The external energy is based on the two-region-based model of "active contours without edges" proposed by Chan and Vese [8]. The Euler-Lagrange equation associated with the minimization of the functional E in equation (1) is shown in equation (2)

$$\begin{aligned} \frac{\partial C}{\partial t} &= \left[\alpha\frac{\partial^2 C}{\partial s^2} - \beta\frac{\partial^4 C}{\partial s^4}\right] \\ &- \left[\lambda_{\text{in}}(I - R_{\text{in}})^2 - \lambda_{\text{out}}(I - R_{\text{out}})^2\right] \text{n}, \quad (2) \end{aligned}$$

where n is the normal unit vector of C pointing outward. The first term is the internal force controlling the smoothness of the contour while the second term is the external force or the region-based force that pushes contour toward the object in the image.

3. DOUBLE REGION-BASED SNAKES

In this paper, we design double region-based snakes to segment the myocardial boundaries of the left ventricle in cardiac MR images. The endocardial and the epicardial boundaries are segmented simultaneously and both active contours are initialized within the epicardial boundary of the left ventricle. We call the first and the second snakes contour A and contour B, respectively. Contour A, located entirely inside contour B, is to segment the endocardial boundary while contour B is to segment the epicardium. With these specifications, we add the inter-contour force to regulate the separation or distance between the two contours. Our energy functional for each of the contours are formulated as in equation (3) and equation (4), respectively,

$$\begin{aligned} E_{\text{A}}(C_{\text{A}}, R_1, R_2) &= \tfrac{1}{2}\int_0^1 \left[\alpha\left(\frac{\partial C_{\text{A}}}{\partial s}\right)^2 + \beta\left(\frac{\partial^2 C_{\text{A}}}{\partial s^2}\right)^2\right] ds \\ &+ \left[\lambda_1 \int_{\overset{\cap}{C_{\text{A}}}} (I - R_1)^2 d\sigma + \lambda_2 \int_{\overset{\cup}{C_{\text{A}}}} (I - R_2)^2 d\sigma\right], \quad (3) \end{aligned}$$

$$\begin{aligned} &E_{\text{B}}(C_{\text{A}}, C_{\text{B}}, R_1, R_3, R_4) = \\ &\tfrac{1}{2}\int_0^1 \left[\alpha\left(\frac{\partial C_{\text{B}}}{\partial s}\right)^2 + \beta\left(\frac{\partial^2 C_{\text{B}}}{\partial s^2}\right)^2\right] ds \\ &+ |R_1 - R_3| \left[\lambda_3 \int_{\overset{\cup}{C_{\text{A}}}\cap\overset{\cap}{C_{\text{B}}}} (I - R_3)^2 d\sigma \right. \\ &\left. + \lambda_4 \int_{\overset{\cup}{C_{\text{B}}}} (I - R_4)^2 d\sigma\right] \\ &+ (D - |R_1 - R_3|)\int_0^1 \left[\nu\left(|C_{\text{B}} - C_{\text{A}}| - r\right)^2\right] ds, \quad (4) \end{aligned}$$

where C_{A} and C_{B} are contours A and B, respectively, I is the local pixel intensity of the image, R_1, R_2, R_3, and R_4 are unknown scalars but to be determined during the evolution process, the constants λ_1, λ_2, λ_3, λ_4, and ν are positive-valued weighting parameters, r and D are positive constants. With calculus of variation, we can see that the energy functional for contour A is similar to equation (1), the single region-based snake. However, we have added the inter-contour energy term, the last term in equation (4), in the functional of contour B in order to ensure a gap between the two contours. The evolution equations associated with the minimization of E_{A} and E_{B} in equation (3) and (4), respectively are:

$$\begin{aligned} \frac{\partial C_{\text{A}}}{\partial t} &= \left[\alpha\frac{\partial^2 C_{\text{A}}}{\partial s^2} - \beta\frac{\partial^4 C_{\text{A}}}{\partial s^4}\right] \\ &- \left[\lambda_1(I - R_1)^2 - \lambda_2(I - R_2)^2\right] \text{n}_{\text{A}}, \quad (5) \end{aligned}$$

and

$$\begin{aligned} \frac{\partial C_{\text{B}}}{\partial t} &= \left[\alpha\frac{\partial^2 C_{\text{B}}}{\partial s^2} - \beta\frac{\partial^4 C_{\text{B}}}{\partial s^4}\right] \\ &- |R_1 - R_3| \left[\lambda_3(I - R_3)^2 - \lambda_4(I - R_4)^2\right] \text{n}_{\text{B}} \\ &- (D - |R_1 - R_3|)\left[2\nu\left(C_{\text{B}} - C_{\text{A}}\right)\left(1 - \frac{r}{|C_{\text{B}} - C_{\text{A}}|}\right)\right], \quad (6) \end{aligned}$$

where n_{A} and n_{B} are the unit outward normal vectors of C_{A} and C_{B}, respectively, R_1 is average pixel intensity of the area inside C_{A}, R_2 is average pixel intensity of the area entirely outside C_{A}, R_3 is average pixel intensity of the area outside C_{A} but inside C_{B}, and R_4 is average pixel intensity of the area outside C_{B}. The graphical representation of these R_i for $i = 1, 2, 3, 4$ is shown in Figure 1 (a).

Form equation (6), the first term is the internal force that regulates the smoothness of the contour, the second term is

the external region-based force that attempts to separate region R_3 form R_4 , and the last term creates the inter-contour force. The inter-contour force controls the distance between each pair of radial points between contour A and contour B as shown in Figure 1(b), creating a band gap of r pixels between the two contours. We can see from equation (6) that the region-based force and the inter-contour force are weighted by $|R_1 - R_3|$ and $D - |R_1 - R_3|$, respectively. The constant D is chosen as an inverse of $|R_1 - R_3|$.

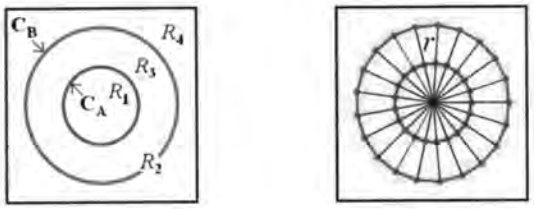

(a) (b)

Fig. 1. (a) Region division of the average intensity in the image and (b) the distance and the relationship of the both contours.

4. EXPERIMENTS

4.1. Synthetic Image

First, we test the performance of our algorithm on a synthetic image resembling the left ventricle of the heart. The 200×200 pixel image is composed of three regions: black region with zero intensity value residing within a grey region of intensity 0.5 on a white background of intensity 1 as shown in Figure 2(a). The two concentric circles in the image's center are the initial contours. We set $r = 15$ pixels and $D = 0.5$. The values for $|R_1 - R_3|$ and $D - |R_1 - R_3|$ are recorded at each iteration and shown in Figure 3(a) and (b), respectively. Initially, when both contours are within the black region, R_1 is equal to R_3, thus the weighting $|R_1 - R_3| = 0$ and $D - |R_1 - R_3| = 0.5$. It means that the influence of the inter-contour force in equation (6) is more than the region-based force, thus the outer contour B is pushed away a distance r pixels from the inner contour A. Figure 2 (b) is the result at the 50^{th} iteration. We observe that the inner contour A is delineating the black region with its own region-based force according to equation (5) but contour B moves pass the back region because of the inter-contour force. Once contour A has traced entirely the black region, the value for R_1, which is the average intensity of the region inside contour A, is zero but the value for R_3, which is the average intensity of the region between the two contours, is approximately 0.5. Therefore, $|R_1 - R_3| \approx 0.5$ and $D - |R_1 - R_3| \approx 0$, which imply a greater influence of the region-based force over the inter-contour force in equation (6). As a result, the outer contour B, from this point on, will extract the grey object with its region-based force. The final segmentation result is shown in Figure 2(c).

(a) (b) (c)

Fig. 2. Performance of double region-based snakes on 200×200 pixel image. (a) The initial position of both contour A and contour B. (b) Result of both contours when at 50^{th} iteration and (c) the final segmentation result.

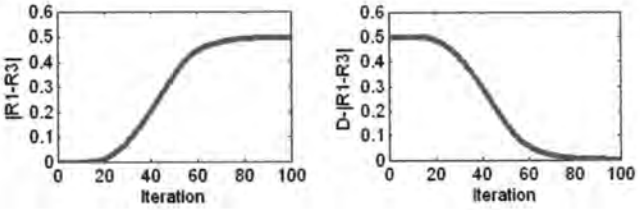

(a) (b)

Fig. 3. (a) Weighting-iteration curves of $|R_1 - R_3|$ and (b) $D - |R_1 - R_3|$ where $D = 0.5$.

We observe that the success in segmentation depends on the r and D parameters set in the evolution equation for contour B. The value for r should be set to be closed to the real distance between the endocardial and epicardial boundaries, and the value for D should be set to be closed to the maximum value for $|R_1 - R_3|$. From the graphs shown in Figure 3(a), we observe that the maximum value $|R_1 - R_3|$ is 0.5. Therefore, the best value for D that causes the value for $D - |R_1 - R_3|$ to be zero at high number of iterations is 0.5 and the graph is shown in Figure 3(b).

4.2. Cardiac MR Images

In this section, we apply our double region-based snakes on a set of real cardiac MR images, which comprise three slices of a human heart: the top, the middle, and the bottom slices, each of size 150×150 pixel. In all three images: (1) the initial position of both contour A and contour B are initialized within the epicardial boundary of left ventricle as shown in Figure 4(a), (b), and (c); and (2) the value for the D parameter is set to 0.35. Due to their different myocardium thicknesses. We set the r parameter in each slice of the cardiac MR images to 18, 12, and 23 pixels, respectively. The papillary muscles problem was solved by checking for convex hull condition on

both active contours at each iteration. When any of the active contours was stuck at the papillary muscles, it is non-convex. Therefore, we add a condition to reinitialize the contour to cover its convex hull, then continue with our double region-based snake algorithm. As a result, the contour moves pass the papillary muscles and successfully segments the endocardial or the epicardial boundary. The final segmentation results are shown in Figure 4(d), (e), and (f), respectively.

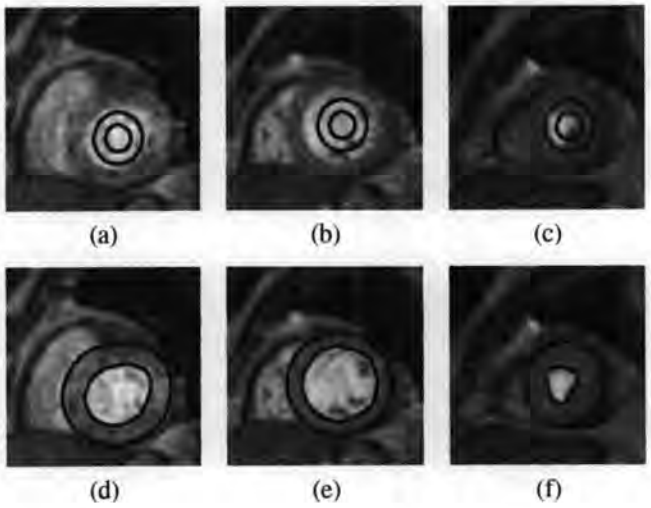

Fig. 4. Performance of double region-based snakes. First row: 150×150 pixel cardiac MR images with initial position of both contour A and contour B. Second row: segmentation results of the endocardial and epicardial boundaries.

We compare our segmentation result with the manual segmentation result using area similarity [13], $S_{area} \in [0, 1]$. The values of the area similarity for the three images in Figure 4(d), (e), and (f) are 0.969, 0.946, and 0.926, respectively.

5. CONCLUSION

In this paper, we proposed double region-based snakes method to segment the endocardial and epicardial boundaries (myocardium boundary) of left ventricle in cardiac MR images simultaneously for 3-D or 4-D heart modeling reconstruction, which is a very useful tool for cardiac diagnosis. The proposed method is based on a region-based parametric active contour, whose performance is better than most edge-based methods. We designed the inter-contour force to control the motion of both active contours so they move toward the endocardial and the epicardial boundaries more accurately. Both contours are initialized within the epicardial boundary of the left ventricle. For the problem of papillary muscles, we solved it by checking for the convex hull condition for both active contours at each iteration. Successful results are shown in both synthetic and real cardiac MR images.

6. ACKNOWLEDGEMENT

This work is partially supported by the grants from Cooperation Project between Department of Electrical Engineering and Private Sector for Research and Development and the Rachadabhisek Sombhoj Chulalongkorn University, Thailand. Moreover, the authors would like to thank Dr. Pairash Saiviroonporn, Dr. Rungroj Krittayaphong, and the Cardiac Center at Siriraj Hospital, Thailand, for providing the MR images.

7. REFERENCES

[1] A. F. Frangi, W. J. Niessen, and M. A. Viergever, "Three-dimensional modeling for functional analysis of cardiac images: A review," *IEEE Transactions on Medical Imaging*, vol. 20, no. 1, pp. 2-25, January 2001.

[2] G. Stalidis, N. Maglaveras, S. N. Efstratiadis, A. S. Dimitriadis, and C. Pappas, "Model-based processing scheme for quantitative 4-D cardiac MRI analysis," *IEEE Transactions on Information Technology in Biomedicine*, vol. 6, no.1, pp. 59-72, March 2002.

[3] M. Lynch, O. Ghita, and P. F. Whelan, "Extraction of epi-cardium contours form unseen images using a shape database," in *Proceedings of Nuclear Science Symposium and Medical Imaging Conference*, vol. 6, pp. 3685-3688, October 2004.

[4] M. Kass, A. Witkin, and D. Terzopoulos, "Snakes: Active contour models," *International Journal of Computer Vision*, vol. 1, no. 4, pp. 321-331, 1988.

[5] C. Xu and J. L. Prince, "Snakes, shapes, and gradient vector flow," *IEEE Transactions on Image Processing*, vol. 7, no. 3, pp. 359-369, March 1998.

[6] J. Cheng and S. W. Foo, "Dynamic directional gradient vector flow for snakes," *IEEE Transactions on Image Processing*, vol. 15, no. 6, pp. 1563-1571, June 2006.

[7] C. Zimmer and J.-C. Olivo-Marin, "Coupled parametric active contours," *IEEE Transactions on Pattern Analysis and Machine Intelligence*, vol. 27, no. 11, pp. 1838-1842, November 2005.

[8] T. F. Chan and L. A. Vese, "Active contours without edges," *IEEE Transactions on Image Processing*, vol. 10, no. 2, pp. 266-277, Febuary 2001.

[9] C. Pluempitiwiriyawej, J. M. F. Moura, Y.-J. L. Wu, and C. Ho, "STACS: New active contour scheme for cardiac MR image segmentation," *IEEE Transactions on Medical Imaging*, vol. 24, no. 5, pp. 593-603, May 2005.

[10] A. Tsai, A. Yezzi, W. Wells, C. Tempany, D. Tucker, A. Fan, W. E. Grimson, and A. Willsky, "A shape-based approach to the segmentation of medical imagery using level sets," *IEEE Transactions on Medical Imaging*, vol. 22, no. 2, pp. 137-154, February 2003.

[11] R.Malladi, J. Sethian, and B. C. Vemuri, "Shape modeling with front propagation: a level set approach," *IEEE Transactions on Pattern Analysis and Machine Intelligence*, vol. 17, no. 2, pp.158-175, February 1995.

[12] C. Pluempitiwiriyawej and S. Sotthivirat, "Active contours with automatic initialization for myocardial perfusion analysis," in *IEEE Proceedings Conference of the Engineering in Medicine and Biology Society (EMBS)*, pp. 3332-3335, September 2005.

[13] A. P. Zijdenbos, B. M. Dawant, R. A. Margolin, and A. C. Palmer, "Morphometric anaysis of white matter lesions in MR images: Method and validation," *IEEE Transactions on Medical Imaging*, vol. 13, no. 4, December 1994.

ประวัติผู้เขียนวิทยานิพนธ์

นายโสภณ ผู้มีจรรยา เกิดวันที่ 13 มกราคม พ.ศ. 2525 ที่จังหวัดนครปฐม สำเร็จการศึกษาระดับปริญญาวิศวกรรมศาสตรบัณฑิต สาขาวิชาวิศวกรรมอิเล็กทรอนิกส์และโทรคมนาคม คณะวิศวกรรมศาสตร์ มหาวิทยาลัยเทคโนโลยีพระจอมเกล้าธนบุรี ในปีการศึกษา 2547 และเข้าศึกษาต่อในหลักสูตรวิศวกรรมศาสตรมหาบัณฑิต ในสังกัดห้องปฏิบัติการวิจัยกรรมวิธีสัญญาณดิจิทัล ภาควิชาวิศวกรรมไฟฟ้า คณะวิศวกรรมศาสตร์ จุฬาลงกรณ์มหาวิทยาลัย ในปีการศึกษา 2548